Pharmacological modulation of glutamatergic and neuroinflammatory pathways in a Lafora disease mouse model

Belén Mollá
Instituto Biomédico de Valencia: Instituto de Biomedicina de Valencia
Miguel Heredia
Instituto de Biomedicina de Valencia
Ángela Campos
Instituto de Biomedicina de Valencia
Pascual Sanz (sanz@ibv.csic.es)
Instituto de Biomedicina de Valencia https://orcid.org/0000-0002-2399-4103

Research Article

Keywords: Lafora disease, cognitive impairment, neuroinflammation, riluzole, memantine, resveratrol, minocycline

Posted Date: February 16th, 2022

DOI: https://doi.org/10.21203/rs.3.rs-1349685/v1

Abstract

Lafora disease (LD) is a fatal rare neurodegenerative disorder that affects young adolescents and has no treatment yet. The hallmark of LD is the presence of polyglucosan inclusions (PGs), called Lafora bodies (LBs), in the brain and peripheral tissues. LD is caused by mutations in either *EPM2A* or *EPM2B* genes, which respectively encode laforin, a glucan phosphatase, and malin, an E3-ubiquitin ligase, with identical clinical presentation. LD knockout mouse models (*Epm2a-/-* and *Epm2b-/-)* recapitulate PGs body accumulation, as in the human pathology, and display alterations in glutamatergic transmission and neuroinflammatory pathways in the brain. In this work, we show the results of four pre-clinical trials based on the modulation of glutamatergic transmission (riluzole and memantine) and anti-neuroinflammatory interventions (resveratrol and minocycline) as therapeutical strategies in an *Epm2b-/-* mouse model. Drugs were administered in mice from 3 to 5 months of age, corresponding early stage of the disease, and we evaluated the beneficial effect of the drugs by *in vivo* behavioral phenotyping and *ex vivo* histopathological brain analyses. The behavioral assessment was based on a battery of anxiety, cognitive, and neurodegenerative tests and the histopathological analyses included a panel of markers regarding PGs accumulation, astrogliosis, and microgliosis. Overall, the outcome of ameliorating the excessive glutamatergic neurotransmission present in *Epm2b-/-* mice by memantine displayed therapeutic effectiveness at the behavioral levels. Modulation of neuroinflammation by resveratrol and minocycline also showed beneficial effects at the behavioral level. Therefore, our study suggests that both therapeutical strategies could be beneficial for the treatment of LD patients.

Introduction

Progressive myoclonus epilepsy of the Lafora type (Lafora disease, LD; OMIM#254780) is an inherited rare neurodegenerative disease of the childhood that courses through intractable epileptic seizures, cognitive decline, and a rapid neurological deterioration until death within ten years from onset [1]. An early feature in LD is the accumulation of insoluble polyglucosan inclusions (PGs) named Lafora bodies (LBs) mainly in the brain [2], [3], which drives symptomatology and remains inalterable throughout the disease. Nowadays, effective treatment is not available yet, neither restorative nor palliative, to delay the progression or alleviate any of the symptoms [4]. In this regard, an enormous collaborative effort has been done within the International Lafora Epilepsy Cure Initiative (LECI) to elucidate an LD therapy or cure [5].

Mutations in either *EPM2A* or *EPM2B/NHLRC1* genes, which respectively encode laforin, a glucan phosphatase, and malin, an E3-ubiquitin ligase, have been described in LD patients [6], [7], [8]. Laforin and malin assemble into a functional complex involved in glycogen metabolism, as part of a quality control mechanism to prevent the accumulation of insoluble glycogen [9], [10]. LD knockout (KO) mouse models with a complete loss of function of laforin (*Epm2a-/-*) [11] or malin (*Epm2b-/-*) [12], [13], [14] partially mimic human symptoms such as early PGs accumulation in muscle, heart, and brain from 2-months of age [11], [14]; they also show slight impairment of motor coordination, abnormal postures of the hindlimb, memory defects and spontaneous myoclonic seizures evident from 9 months of age [11], [14], [15]; finally,

they present enhanced excitability [11] with hyperactive behavior from 1 to 11-month-old [16], [17]. At the histopathological level, the brain of LD mouse models shows neurodegeneration with loss of GABAergic and parvalbumin+ (PV+) neurons and dendritic abnormalities in pyramidal neurons [16], [17], [18], massive astrogliosis accumulating PGs [19], [20], as well as an early neuroinflammatory status from 3 months of age [21], [22].

Since astrocytic functionality seems to be compromised in LD mouse models, our laboratory has studied the possible alterations in excitatory glutamatergic transmission to gain insight into the glutamatergic system, as an essential regulator of epileptic seizures. Successfully, Muñoz-Ballester et al [23] unraveled a decreased level of glutamate transporter GLT-1 at the plasma membrane of LD astrocytes, which might underlie the *in vivo* glutamate clearance defects present in LD mouse models [24]. Furthermore, Perez-Jimenez et al [25] confirmed that such defective alterations are related to insufficient ubiquitination of GLT-1 due to the absence of a functional laforin/malin complex. On the strength of these data, it became clear that an altered excitatory glutamatergic system might be behind the sensitivity to convulsant agents observed in LD mouse models [26], [27]. Recently, our laboratory has also been involved in defining neuroinflammation as a novel hallmark of LD. In this regard, we have described progressive neuroinflammation in the brain of LD mice which increasingly worsens from 3 to 16 months of age [22].

The work we present in this manuscript is an extension of the previous achievements of our laboratory in preclinical studies in LD by using metformin [28], which led to the designation of metformin as an orphan drug for the treatment of Lafora disease by the European Medicines Agency (EMA) and the USA Food and Drug Administration (FDA). In addition, we have recently reported the beneficial effect of the administration of propranolol, not only in memory and attention defects but also in the accumulation of polyglucosan inclusions, neuronal disorganization, astrogliosis, and microgliosis in the hippocampus of LD mice [29]. Following this line of work, and to repurpose further drugs for LD, in this work we have carried out four novel pre-clinical studies in *Epm2b-/-* mice with two different strategies of intervention based on targeting glutamatergic transmission (riluzole and memantine) as well as neuroinflammation (resveratrol and minocycline).

Riluzole is the first FDA-approved medication for amyotrophic lateral sclerosis (ALS) due to its capability to modulate glutamate neurotransmission by inhibiting both presynaptic glutamate release and postsynaptic glutamate receptor signaling [30]. Riluzole has been effective in delaying median time to death in a mouse model of ALS [31] and cognitive decline in Alzheimer's Disease (AD) mouse models [32], [33]. On the other hand, memantine is an antagonist of postsynaptic glutamate NMDA receptors, which reduces the effects of excitotoxic glutamate release. This compound is regularly prescribed to improve the cognitive impairments in AD [34], [35].

Resveratrol is known worldwide as a nutraceutical by its anti-oxidative, anti-aging, and anti-inflammatory properties [36], [37], but it also has been recognized as a promising therapeutic agent against chronic neuroinflammation and neurodegeneration in AD [38], [39]. In the same light, minocycline, a classical

tetracycline antibiotic, has also been reported with novel anti-inflammatory and neuroprotective activities in several neurodegenerative conditions such as ALS, AD, or Huntington's disease [40], [41].

In this work, we have administered these compounds to 3-month-old *Epm2b-/-* mice (corresponding to early stages of LD) for two months. We have analyzed neurodegenerative status and cognitive tasks (memory and anxiety-like behavior) in these mice, as well as histopathological hallmarks in the brain [presence of polyglucosan inclusions (PGs), microgliosis, and astrogliosis] to evaluate the effectiveness of all pharmacological interventions. We found an improvement in the performance of behavioral tests and an amelioration of neurodegenerative signs by modulating neuroinflammation with resveratrol and minocycline and also by promoting neuroprotection with memantine. In the case of riluzole, we did not find any significant beneficial effect. Therefore, the results presented in this work support the potential beneficial effects of both interventional strategies in LD.

Material And Methods

Animals

Malin knockout mice (*Epm2b-/-*) on a pure C57BL/6JRccHsd background and the corresponding control mice (WT) [29] were maintained at the IBV-CSIC facility on a 12 light/dark cycle with food and water *ad libitum*. A total of 63 WT and 93 *Epm2b-/-* male mice were randomly assigned to untreated or treated groups along with four different pre-clinical trials (riluzole, memantine, resveratrol, and minocycline). The number of animals per group for each trial was as follow: 1) vehicle group (N=7 WT and N=6 *Epm2b-/-* mice) and treated group (N=11 WT and N=11 *Epm2b-/-* mice) for the riluzole study; 2) vehicle group (N=15 WT and N=15 *Epm2b-/-* mice) and treated group (N=15 WT and N=15 *Epm2b-/-* mice) for the resveratrol study; and 3) vehicle group (N=15 WT and N=15 *Epm2b-/-* mice) and treated group for memantine and minocycline study (N=15 *Epm2b-/-* mice for each drug). The vehicle groups were administered with the corresponding vehicle used in the treated groups. Since no gender-link phenotype has been reported in mice or humans for Lafora disease, we used male mice to compare the results with previous data obtained in the lab.

Drugs and administration

All drugs tested in this work, riluzole (R116), memantine (M9292), and minocycline (M9511) were obtained from Sigma-Aldrich and trans-resveratrol (3,40,5-trihydroxy trans-stilbene, 70675) from Cayman chemicals. Different pre-clinical trials were designed based on both the pathway (oral or intraperitoneal injection) and the drug solvent of the administration (water, saline, or vehicle). Thus, three pre-clinical trials were performed separately and consecutively: 1) the riluzole study was performed by oral administration in drinking water; 2) the resveratrol trial by intraperitoneal administration using vehicle solution (4% ethanol, 75 mM NaCl, 2.5% PEG4000, and 2.5% Tween20); and finally, 3) the memantine and minocycline assay by intraperitoneal administration in saline solution. Animals of three months of age either received riluzole (10 mg/Kg/day) in drinking water or were injected intraperitoneally with vehicle solution alone or containing resveratrol (12 mg/Kg), or with saline solution alone or containing

memantine (25 mg/Kg) or minocycline (25 mg/Kg), in a volume of 100 µl, three times per week, during two months. Drug doses were based on a bibliographic search for all of them: riluzole [42], [43], resveratrol [44], [45], memantine [46], and minocycline [47]. These previous studies concluded that the doses we used in our assays were safe and that all compounds reached the brain to exert their effects.

Behavioral tests

After a 2-month treatment, animals were subjected to a battery of behavioral tests conducted during the light phase from 8:00 am to 3:00 pm. The order of the behavioral tests and resting time between them were the same for each mouse. The battery of behavioral tests consisted of five tests performed in the following order: hindlimb clasping, open field, elevated plus maze, Y-maze, and Object Location Memory (OLM). Tests were conducted in order of increasing invasiveness: reflecting action, anxiety, and memory. Mice rested 48-72 hours between tests (Supplementary Fig. S1). Behavioral tests were recorded by using the SMART Video Tracking software from PanLab/Harvard Apparatus to evaluate mouse movement. This advanced image analysis allows the recording of activity, trajectories, and a wide variety of standard calculations related to tracking such as time/distance/entries in zones both by user-defined zones and by the entire area of mazes. We used the following tests:

- Hindlimb clasping: Hindlimb clasping scores abnormal postures related to neurodegeneration and has been used as a marker of disease progression in a large number of neurodegenerative mouse models [48]. Mice were grasped by their tail for 10 seconds and hindlimb positions were scored from 0 to 3 [49]. If the hindlimbs were consistently splayed outward, away from the abdomen, it was assigned a score of 0 (absence). If one or two hindlimbs were partially retracted toward the abdomen for more than 5 seconds, it received a score of 1 (mild) or 2 (moderate), respectively. If both hindlimbs were completely retracted toward the abdomen it received a score of 3 (severe).

- Open Field maze: The Open Field test is used to assess anxiety and exploratory behaviors [50]. Mice were placed in the middle of a peripheral zone of the arena (a wall-enclosed 50cm x 50cm area) facing the wall and allowed to explore freely for 5 minutes. We analyzed the distance walked in peripheral and center areas (40% of the total surface of the area), as well as the total number of entries into the center. As anxiety levels rise, the animal tends to remain close to walls in the peripheral zone, avoiding entry into the central zone which is considered more anxiogenic.

- Elevated plus maze: The elevated plus maze was used to evaluate anxiety-related behavior in mice [51]. Mice were placed in the intersection of the four arms of the elevated plus maze and their free movement was recorded for 5 minutes. The elevated plus maze has two open arms and two close arms with walls. The time spent in open and closed arms was measured, as well as the total number of arm entries made. The tendency of a subject to remain close to walls increases as anxiety levels rise, avoiding entry and the spent of time in open arms.

- Y-maze: To evaluate non-hippocampal short-term working memory we performed the Y-maze test as previously detailed in [29]. % spontaneous alternations and % incomplete spontaneous alternations were

determined.

- Object location memory (OLM): To evaluate spatial recognition memory depending on the hippocampus we performed OLM probe as previously detailed in [29]. Discrimination index (DI) and activity time were measured.

Tissue collection and histopathological analyses

Animals were euthanized by cervical dislocation; brains were removed, and the right hemisphere was immediately fixed in 4% paraformaldehyde (PAF) at 4ºC overnight and embedded in paraffin for histological analyses. Five µm paraffin sagittal sections were obtained by microtome and sections were deparaffinized and hydrated with deionized water. The detection of PGs by periodic acid Schiff (PAS) staining and immunohistochemical analysis were performed as detailed in [29]. For immunohistochemistry, primary and secondary antibodies used were: guinea pig anti-GFAP (1:500, Synaptic Systems #173_004), rabbit anti-Iba1 (1:200, WAKO #019-19741), Alexa Fluor-conjugates [1:500, Life Technologies: goat anti-guinea pig IgG Alexa Fluor® 594 (#A11076), and goat anti-rabbit IgG Alexa Fluor® 488 (#A11008)]. Background controls of secondary antibodies were performed in parallel. Nuclear staining was performed with DAPI (Sigma-Aldrich). Coverslips were mounted with Fluoromount-G™ (Thermo Fisher Scientific).

Image acquisition and analysis

Two sections per animal with a 24-µm-gap between them were analyzed. Three pictures per section were taken in different hippocampal areas: Cornus Ammonis (CA1), molecular layer of CA1 plus DG (CA1-DG), and dentate gyrus (DG). PAS staining photomicrographs were acquired using a Leica DM RXA2 microscope for the riluzole study or using a Leica DM750 microscope (Nussloch, Germany) for resveratrol, memantine, and minocycline trials, connected to a Hamamatsu color camera with an X40 magnification in RGB format. Immunofluorescence images were acquired using a Leica TCS Sp8 laser-scanning confocal microscope with an X40 objective for the riluzole study or by a Leica DM6 B automatic microscope connected to a Leica k5 monochrome high sensibility camera with an X20 objective for resveratrol, memantine, and minocycline trials. 10-12 z-axis stacks separated by 0.33 µm were taken per section and 2D reconstruction was projected as maximum intensity using ImageJ software (NIH, Bethesda, MD, USA).

For automated computer image analysis, we used the programmed tailored macros in ImageJ for PAS and fluorescence histological detection as detailed in [29].

Data analysis

Statistical analysis was performed with RStudio R-4.0.3 [52]. Quantitative data were represented as mean ± standard error of the mean (SEM) with a 95% confidence interval. The normality of the data was analyzed by the Shapiro-Wilk test and homogeneity of variance by the Levene test. To assess the statistical significance (p-value) of the effects in multiple comparisons, data with a normal distribution

were analyzed by two-way ANOVA followed by a Tukey's post hoc test. Non-parametric data were analyzed by Kruskal-Wallis followed by Dunn's test. To assess the effect size of the interventions in multiple comparisons, Cohen's delta coefficient (d) was calculated and scored as negligible (d < 0.20), small (d≥0.20), medium (d≥0.50), large (d≥0.80), and much larger (d≥1.00) size effect [53], [54]. A descriptive and inferential statistical summary of analyzed behavioral and histopathological variables is supplied (see Supplementary Table S1 and Table S2). A critical value for significance of *p < 0.05 was used throughout the study.

Results

In this work, we have evaluated the efficacy of the treatment of *Epm2b-/-* mice with four drugs, two of them previously used as glutamatergic modulators (riluzole and memantine) and the other two used as neuroinflammatory-modifying therapeutic agents (resveratrol and minocycline). Treatments were administered in male mice of 3 months of age (corresponding to an early stage of LD) for two months. After treatments, we performed an *in vivo* analysis of anxiety-like, cognitive behavior and neurodegenerative signs followed by an *ex vivo* histopathological analysis of PG inclusions, astrogliosis, and microgliosis in the corresponding mouse brains. For the sake of clarity, we present the results as independent treatments (although memantine and minocycline were performed at the same time since they shared the same vehicle), comparing the values of treated *Epm2b-/-* mice to *Epm2b-/-* mice that received only water, vehicle, or saline, respectively.

Decreased anxiety-like and hyperactive behavior of *Epm2b-/-* mice are attenuated by anti-neuroinflammatory treatments

The anxiety-like behavior was evaluated in *Epm2b-/-* mice at 5 months of age by carrying out Open Field and Elevated Plus maze tests. In the Open File test, the percentage of traveled distance in the center and the number of entries into the center were measured as key indicators of anxiety and hyperactivity, respectively. Untreated *Epm2b-/-* mice showed a tendency not only to travel more distance in the center zone (Fig. 1) [e.g., *Epm2b-/-* (26.17 ± 2.49) and WT (19.97 ± 2.13, p=0.073, d=-0.71 medium) (Fig. 1C)] but they also made a greater number of entries into the center [e.g., *Epm2b-/-* (21.92 ± 2.53) and WT (16.92 ± 2.19, p=0.239, d=-0.56 medium) (Table S1)]. Although not statistically significant, both behaviors pointed out a tendency to decrease anxiety and hyperactive behavior in *Epm2b-/-* mice, as already reported by other authors [16], [17]. After the anti-inflammatory treatments (resveratrol and minocycline), the % traveled distance of *Epm2b-/-* in the center was decreased significantly by resveratrol (14.64 ± 2.15, p=0.011*, d=0.80 large) (Fig. 1D) and minocycline (18.01 ± 2.24, p=0.032*, d=0.95 large) (Fig. 1E), in comparison to the corresponding *Epm2b-/-* mice treated with the respective vehicle, normalizing its anxiety levels up to control levels (Fig. 1D and 1E). In contrast, riluzole (24.71 ± 2.34, p=0.896, d=0.38 small) (Fig. 1B) and memantine (24.36 ± 2.79, p=0.593, d=0.17 negligible) (Fig. 1C) had only a minor effect on this parameter. Regarding the number of entries into the center, only minocycline was capable to decrease this parameter significantly (9.63 ± 1.47, p=0.0017**, d=1.57 much large) up to control levels (Table S1).

We used the Elevated Plus Maze as an alternative method to confirm the low anxiety and hyperactivity present in *Emp2b-/-* mice. We observed the same abnormal behavior in *Epm2b-/-* mice, which showed a slight increase in the number of entries into arms (38.53 ± 4.38) than WT (32.93 ± 4.23, p=0.310, d=-0.33 small) (Table S1), confirming reduced anxiety and hyperactive behavior. None of the treatments were able to modify the *Epm2b-/-* mice behavior in the elevated plus maze test (Table S1), except for minocycline which significantly decreased the number of entries into arms (25.33 ± 3.33, p=0.050*, d=0.87 large) compared to *Epm2b-/-* treated with the corresponding vehicle. Therefore, minocycline was the only effective treatment to control the hyperactive behavior of *Epm2b-/-* mice in both anxiety tests, Open Field and Elevated Plus Maze.

Attention defect in *Epm2b-/-* mice is improved by memantine and minocycline treatments

The cognitive profile of *Epm2b-/-* mice was evaluated at 5 months of age by assessing working memory, and short-term location memory. To evaluate working memory, animals were tested for the % spontaneous alternations in the Y-maze (Table S1), and % incomplete alternations were quantified (Fig. 2). Regarding % spontaneous alternations, although a repeated tendency to a slight decrease of this parameter in untreated *Epm2b-/-* mice compared to WT was present through the trials (Table S1), we concluded that *Epm2b-/-* mice did not display any working memory defect due to the absence of either statistical significance (p-value) or large effect size (d) in the means, in agreement with previously published results [29]. In contrast, % incomplete alternations were increased in untreated *Epm2b-/-* compared to WT mice (Fig. 2) (e.g., 40.38 ± 7.40 in *Epm2b-/-* mice vs 15.03 ± 5.90, in WT mice; p=0.017*, d=-0.97 large; Fig. 2C), suggesting an attention defect in ending the task. Interestingly, the % incomplete alternations in *Epm2b-/-* mice were significantly decreased by memantine (19.11 ± 6.18, p=0.035*, d=0.80 medium) and minocycline (20.46 ± 6.06, p=0.0780, d=0.80 medium), suggesting a positive effect of memantine and minocycline in improving the staying on-task of exploration.

More related to hippocampal memory, we studied spatial short-term memory using the object location memory test (OLM) (Fig. 3). The discrimination index (DI) of object location and the total activity time were measured. There were no significant differences (p-value) or remarkable effect size (d) in DI among all the groups (Table S1), suggesting that short-term location memory was not affected in *Epm2b-/-* mice at 5 months of age, in agreement with previous results [29]. However, we noticed a tendency to an increase in the total activity time in *Emp2b-/-* compared to WT in untreated animals (e.g., 196.86 ± 14.10 sec in Epm2b-/- mice vs 157.00 ± 12.22 sec in WT mice; p=0.048*, d=-0.77 medium; Fig. 3C), highlighting again the hyperactive behaviour in *Epm2b-/-* mice. Among the treatments, we nicely observed that only memantine treatment significantly decreased the total activity time in *Epm2b-/-* mice (145.26 ± 15.73 sec, p=0.016*, d=-0.89 large) (Fig. 3C), reducing hyperactive behavior.

Neurodegenerative signs detected in 5-month-old *Epm2b-/-* mice are ameliorated by memantine, resveratrol, and minocycline treatments

Epm2b-/- mice were evaluated for abnormal postures related to neurodegeneration by using the hindlimb clasping test. In untreated *Epm2b-/-* mice at 5 months of age the hindlimb clasping score was

significantly and repeatedly worse in all trials compared to WT (Fig. 4A-D) (Table S2). Among the treatments, we observed a significant improvement after memantine (p=0.0007***) (Fig. 4B), resveratrol (p=1.63e-07****) (Fig. 4C), and minocycline (p=4.73e-09****) (Fig. 4D) treatments. Therefore, neurodegenerative signs present in *Epm2b-/-* mice were ameliorated by these pharmacological treatments. However, riluzole treatment worsened the neurodegenerative signs (p=2.14e-10****) (Fig. 4A) (Table S2).

Only glutamatergic modulators have a minor effect on the formation of polyglucosan inclusions in *Epm2b-/-* mice

To evaluate the presence of PGs inclusions in mice, brain slices were obtained and stained with a periodic acid-Schiff stain (PAS) which detects polysaccharides such as glycogen. The number of PGs per 10,000 µm2 was quantified by image analysis as indicated in the Materials and Methods section and the percentages of PGs number *versus* untreated *Epm2b-/-* mice were plotted on a graph. Representative pictures of PAS staining (Fig. 5A) disclosed an enormous number of PGs in *Epm2b-/-* compared to WT mice (e.g., 100.00 ± 17.31 in *Epm2b-/-* mice vs 1.18 ± 0.77 in WT mice; p=0.0099**, d=-2.75 much large; Fig. 5B), which was significantly repeated through all trials (Fig. 5B-E) (Table S1). This greater number of PGs was ameliorated by 40% in riluzole (60.23 ± 9.26, p=0.260, d=1.13 much large) and by 15% in memantine (84.76 ± 8.79, p=0.264, d=0.88 large) treated *Epm2b-/-* mice (Fig. 5B-C) compared to *Epm2b-/-* mice treated with the corresponding vehicle, albeit it was not statistically significant. Even though not being significant, the effect size (Cohen's coefficient) of the reduction in the PGs number was much large for riluzole and large for memantine treatments, suggesting a positive reduction. Thus, we consider that two-month glutamatergic treatments might have, if any, only a minor effect preventing the formation of PG inclusions in *Epm2b-/-* mice. On the contrary, anti-neuroinflammatory treatments did not affect PGs accumulation (resveratrol 98.34 ± 8.58, p=0.864, d=0.05 negligible; minocycline 98.03 ± 4.51, p=0.780, d=0.17 negligible) (Fig. 5D-E) (Table S1).

Reactive astrogliosis in *Epm2b-/-* mice is not modulated by any of the pharmacological treatments

Since we have found that the accumulation of PGs is significantly correlated to the appearance of reactive astroglia and microglia in *Epm2b-/-* mice [29], we examined reactive astrogliosis in *Epm2b-/-* mice. We detected the astrocytic marker GFAP (in magenta), and the nuclear marker DAPI (in blue) by immunofluorescence (Fig. 6A). As described previously [28], [21], [29], untreated *Epm2b-/-* showed a massive GFAP+ area compared to WT mice (Fig. 6A) (e.g., 100.00 ± 9.57 in *Epm2b-/-* mice vs 38.98.15 ± 7.05 in WT mice; p=0.0062**, d=-2.96 much large; Fig. 6C) (Table S1), which suggests a remarkable pathological reactive astrogliosis in the brain of *Epm2b-/-* mice. Unfortunately, neither riluzole (Fig. 6B), nor memantine (Fig. 6C), nor resveratrol (Fig. 6D) nor minocycline (Fig. 6E) treatments significantly modified the affectation of astrogliosis in the brain of *Epm2b-/-* mice (Table S1).

Only riluzole treatment has a minor effect on the microgliosis in *Epm2b-/-* mice

Finally, we detected the microglial marker Iba1 (in gray) by immunofluorescence (Fig. 7A) and the number of Iba1+ cells with clear changes in morphology was counted as a marker of microglial activation [55]. We confirmed an increase in activated microglia in untreated *Epm2b-/-* (100.00 ± 11.48) compared to WT (77.18 ± 4.49, p=0.543, d=-0.94 large) (Fig. 7) (Table S1). Riluzole was the only pharmacological treatment capable to decrease the number of altered microglia in *Epm2b-/-* (71.75 ± 4.82, p=0.090, d=1.21 much large) down to control levels. In contrast, memantine (Fig. 7C), resveratrol (Fig. 7D), and minocycline (Fig. 7E) did not affect the number of reactive microglia (Table S1).

Discussion

Lafora disease (LD) is a fatal rare neurological disorder that leads to the death of patients around 10 years from onset. Work is underway to develop drugs that could be used as a cure or as disease-modifying agents. These strategies have been aimed to reduce the formation of LB's by inhibiting glycogen synthase (GYS1) activity, either by using antisense oligonucleotides (ASOs) [56] or by small chemical compounds that inhibit GYS1 [57]. Moreover, one approach was designed to digest LB's by using an antibody-enzyme fusion [58] [59]. In addition, alternative strategies aimed to ameliorate the symptoms of LD have been implemented in LD mouse models. For example, a ketogenic diet has been recently described as being useful in reducing the formation of LB's [60], and our group has described the use of repurposing drugs that ameliorate LD pathophysiology. In this sense, we reported that metformin has a beneficial effect on *Epm2b-/-* mice [28] and these results allowed the designation of this compound as an orphan drug for the treatment of LD, both by the European Medicines Agency (EMA/3/16/1803) and the Food and Drug Administration (FDA/#17-6161). Recently, we described that the use of modulators of neuroinflammation had also a beneficial effect in *Epm2b-/-* mice, especially propranolol that reduced the formation of reactive glia and had amelioration of different behavioral tests [29].

In this work, we have expanded our analysis to additional repurposing drugs focusing our attention on compounds that affect either glutamatergic transmission or neuroinflammation. As an example of the first, we used riluzole and memantine. Riluzole is the first FDA-approved medication for amyotrophic lateral sclerosis (ALS) due to its capability to modulate glutamate neurotransmission, not only by inhibiting presynaptic glutamate release but by enhancing the clearance of this neurotransmitter by astrocytic glutamate transporters, which results in a reduction of postsynaptic glutamate receptor signaling [30]. We found that riluzole did not have a major effect on the behavioral tests described in this study, except that it worsened the neurodegenerative-related hindlimb clasping test. At the histopathological level, riluzole decreased the number of PGs by 40% and the number of reactive microglia, although in both cases the differences were not statistically significant (Table 1).

In the case of memantine, an antagonist of postsynaptic glutamate NMDA receptors, which reduces the effects of excitotoxic glutamate release, we found a statistically significant beneficial effect of this drug on several behavioral tests related to exploration behavior (incomplete alternancies in Y-maze), hyperactivity (OLM activity time) and neurodegenerative signs (hindlimb clasping). These beneficial effects were not related to the levels of PGs or reactive glia (Table 1), suggesting that the positive effect

of memantine could be due to the inhibition of post-synaptic NMDA receptor signaling. It is worth pointing out that the excitotoxicity associated with the overactivation of this receptor may cause neuronal death and cognitive deficits associated with dementia such as learning and memory impairments [35]. Moreover, in several clinical assays, memantine monotherapy was found to exert efficacy on hyperactivity and attention deficit in adult patients with attention deficit hyperactivity disorder (ADHD) [61]. Therefore, the beneficial effects of memantine on the cognitive and behavioral profile of *Epm2b-/-* mice are likely due to an amelioration of the excitotoxicity produced by imbalanced glutamate levels present in these mice [24]. In this sense, the effects of memantine would be analogous to the beneficial effects obtained with perampanel, an inhibitor of post-synaptic glutamate AMPA receptors [62]. Probably, the beneficial effects of both compounds are due to a decrease in neuronal hyperexcitability due to a downregulation of the activity of the postsynaptic glutamate receptors AMPA (by perampanel) [63] and NMDA (by memantine) (this work).

To modulate neuroinflammation, we used resveratrol and minocycline. It has been reported that resveratrol has anti-oxidative, anti-aging, and anti-inflammatory properties [36], [37]. In *Epm2b-/-* mice, this compound had a beneficial effect on some behavioral tests related to anxiety (open field) and neurodegenerative signs (Hindlimb clasping). However, resveratrol did not affect the levels of PGs or the levels of reactive glia (Table 1). Perhaps, the beneficial effect of resveratrol could be related to alternative pathways, since it has been described that resveratrol decreases the production of pro-inflammatory cytokines via the activation of AMP-activated protein kinase (AMPK), SIRT1, and SOCS1, and also reduces reactive oxygen species (ROS) production [64], [65].

Finally, we used minocycline, a tetracycline antibiotic derivative that has anti-inflammatory and neuroprotective activities in several neurodegenerative conditions [40], [41]. In *Epm2b-/-* mice we found a beneficial effect of this compound on different behavioral tests related to anxiety (open field), exploration behavior (incomplete alternancies in Y-maze), and neurodegenerative signs (hindlimb clasping). However, this drug did not affect the levels of PGs and, surprisingly, it did not reduce the levels of reactive glia (Table 1), suggesting that minocycline had affected alternative pathways. In this sense, it is worth noting that, in addition to its anti-inflammatory properties, minocycline prevents neurons from glutamate toxicity as this compound reduces the release of glutamate and the excitability of neurons in the hippocampus [66], represses the expression of the NR2A subunit of the NMDA receptor [47], attenuates NMDA-induced Ca++ entry and excitotoxicity [67], and ameliorated downregulation of glial glutamate transporters expression promoting glutamate uptake in the spinal sensory synapses [68]. Therefore, the beneficial effects of minocycline on the cognitive and behavioral profile of *Epm2b-/-* mice are likely due to an amelioration of neuronal excitotoxicity, resembling the memantine treatment described above.

In summary, among the four different compounds analyzed in this work, selected to modify either the altered glutamatergic transmission or the neuroinflammation profiles present in *Epm2b-/-* mice, memantine (an inhibitor of the post-synaptic NMDA receptors) and minocycline (an antibiotic derivative with broad physiological functions) were the most promising candidates to be considered, either alone or in combination with other repurposing drugs, in future therapeutic strategies for LD. It is interesting to

point out that, despite targeting initially both pathways separately, we obtained interlinked pharmacological effects between them, mainly related to amelioration of glutamate-induced excitotoxicity. This highlights the importance of the altered glutamatergic transmission in the development of the pathophysiological symptoms of LD.

Declarations

Funding

This work was supported by a grant from the Spanish Ministry of Science and Innovation PID2020-112972RB-I00, an intramural grant ACCI2020 from CIBERER, and a grant from the National Institutes of Health P01NS097197, which established the Lafora Epilepsy Cure Initiative (LECI), to P.S.

Competing interests

The authors declare that they have no competing interests

Ethics approval and consent to participate

All animal experiments were approved by the animal committee of the Instituto de Biomedicina de Valencia-CSIC [Permit Number: INTRA12 (IBV-4)] and carried out in accordance with recommendations for the Care and Use of Laboratory Animals of the Consejo Superior de Investigaciones Cientificas (CSIC, Spain).

Consent to participate

Not applicable

Consent for publication

Not applicable

Availability of data and materials

All data generated or analyzed during this study are included in this published article and its supplementary information files.

Code availability

Not applicable

Authors' contributions

MH, AC and BM performed all experiments. BM analyzed and interpreted the data and participated in the writing of the manuscript. PS interpreted the data and participated in the writing of the manuscript. All

authors have read and approved the final manuscript.

ACKNOWLEDGMENTS

We want to thank Dr. Maria Adelaida Garcia-Gimeno for the critical reading of the manuscript and the people in charge of the IBV animal house facility for their help in managing all the animals.

References

1. Turnbull J, Tiberia E, Striano P, Genton P, Carpenter S, Ackerley CA, Minassian BA (2016) Lafora disease. Epileptic Disord 18(S2):38–62
2. Lafora GR, Glueck B (1911) Beitrag zur histogpathologie der myoklonischen epilepsie. Gesamte Neurol Psychiatr 6:1–14
3. Sakai M, Austin J, Witmer F, Trueb L (1970) Studies in myoclonus epilepsy (Lafora body form). II. Polyglucosans in the systemic deposits of myoclonus epilepsy and in corpora amylacea. Neurology 20(2):160–176
4. Mitra S, Gumusgoz E, Minassian BA (2021) Lafora disease: Current biology and therapeutic approaches. Rev Neurol (Paris). doi:10.1016/j.neurol.2021.06.006
5. Markussen KH, Macedo JKA, Machio M, Dolce A, Goldberg YP, Vander Kooi CW, Gentry MS (2021) The 6th International Lafora Epilepsy Workshop: Advances in the search for a cure. Epilepsy Behav 119:107975
6. Minassian BA, Lee JR, Herbrick JA, Huizenga J, Soder S, Mungall AJ, Dunham I, Gardner R, Fong CY, Carpenter S, Jardim L, Satishchandra P, Andermann E, Snead OC 3, Lopes-Cendes I, Tsui LC, Delgado-Escueta AV, Rouleau GA, Scherer SW (1998) Mutations in a gene encoding a novel protein tyrosine phosphatase cause progressive myoclonus epilepsy. Nat Genet 20(2):171–174
7. Serratosa JM, Gomez-Garre P, Gallardo ME, Anta B, de Bernabe DB, Lindhout D, Augustijn PB, Tassinari CA, Malafosse RM, Topcu M, Grid D, Dravet C, Berkovic SF, de Cordoba SR (1999) A novel protein tyrosine phosphatase gene is mutated in progressive myoclonus epilepsy of the Lafora type (EPM2). Hum Mol Genet 8(2):345–352
8. Chan EM, Young EJ, Ianzano L, Munteanu I, Zhao X, Christopoulos CC, Avanzini G, Elia M, Ackerley CA, Jovic NJ, Bohlega S, Andermann E, Rouleau GA, Delgado-Escueta AV, Minassian BA, Scherer SW (2003) Mutations in NHLRC1 cause progressive myoclonus epilepsy. Nat Genet 35(2):125–127
9. Garcia-Gimeno MA, Knecht E, Sanz P (2018) Lafora Disease: A Ubiquitination-Related Pathology. Cells 7(8):8
10. Nitschke F, Ahonen SJ, Nitschke S, Mitra S, Minassian BA (2018) Lafora disease - from pathogenesis to treatment strategies. Nat Rev Neurol 14(10):606–617
11. Ganesh S, Delgado-Escueta AV, Sakamoto T, Avila MR, Machado-Salas J, Hoshii Y, Akagi T, Gomi H, Suzuki T, Amano K, Agarwala KL, Hasegawa Y, Bai DS, Ishihara T, Hashikawa T, Itohara S, Cornford EM, Niki H, Yamakawa K (2002) Targeted disruption of the Epm2a gene causes formation of Lafora

inclusion bodies, neurodegeneration, ataxia, myoclonus epilepsy and impaired behavioral response in mice. Hum Mol Genet 11(11):1251–1262

12. DePaoli-Roach AA, Tagliabracci VS, Segvich DM, Meyer CM, Irimia JM, Roach PJ (2010) Genetic depletion of the malin E3 ubiquitin ligase in mice leads to lafora bodies and the accumulation of insoluble laforin. J Biol Chem 285(33):25372–25381
13. Turnbull J, Wang P, Girard JM, Ruggieri A, Wang TJ, Draginov AG, Kameka AP, Pencea N, Zhao X, Ackerley CA, Minassian BA (2010) Glycogen hyperphosphorylation underlies lafora body formation. Ann Neurol 68(6):925–933
14. Criado O, Aguado C, Gayarre J, Duran-Trio L, Garcia-Cabrero AM, Vernia S, San Millan B, Heredia M, Roma-Mateo C, Mouron S, Juana-Lopez L, Dominguez M, Navarro C, Serratosa JM, Sanchez M, Sanz P, Bovolenta P, Knecht E, de Rodriguez S (2012) Lafora bodies and neurological defects in malin-deficient mice correlate with impaired autophagy. Hum Mol Genet 21(7):1521–1533
15. Garcia-Cabrero AM, Marinas A, Guerrero R, de Cordoba SR, Serratosa JM, Sanchez MP (2012) Laforin and malin deletions in mice produce similar neurologic impairments. J Neuropathol Exp Neurol 71(5):413–421
16. Valles-Ortega J, Duran J, Garcia-Rocha M, Bosch C, Saez I, Pujadas L, Serafin A, Canas X, Soriano E, Delgado-Garcia JM, Gruart A, Guinovart JJ (2011) Neurodegeneration and functional impairments associated with glycogen synthase accumulation in a mouse model of Lafora disease. EMBO Mol Med 3(11):667–681
17. Taneja K, Ganesh S (2021) Dendritic spine abnormalities correlate with behavioral and cognitive deficits in mouse models of Lafora disease. J Comp Neurol 529(6):1099–1120
18. Ortolano S, Vieitez I, Agis-Balboa RC, Spuch C (2014) Loss of GABAergic cortical neurons underlies the neuropathology of Lafora disease. Mol Brain 7:7
19. Rubio-Villena C, Viana R, Bonet J, Garcia-Gimeno MA, Casado M, Heredia M, Sanz P (2018) Astrocytes: new players in progressive myoclonus epilepsy of Lafora type. Hum Mol Genet 27(7):1290–1300
20. Auge E, Pelegri C, Manich G, Cabezon I, Guinovart JJ, Duran J, Vilaplana J (2018) Astrocytes and neurons produce distinct types of polyglucosan bodies in Lafora disease. Glia 66(10):2094–2107
21. Lopez-Gonzalez I, Viana R, Sanz P, Ferrer I (2017) Inflammation in Lafora Disease: Evolution with Disease Progression in Laforin and Malin Knock-out Mouse Models. Mol Neurobiol 54(5):3119–3130
22. Lahuerta M, Gonzalez D, Aguado C, Fathinajafabadi A, Garcia-Gimenez JL, Moreno-Estelles M, Roma-Mateo C, Knecht E, Pallardo FV, Sanz P (2020) Reactive Glia-Derived Neuroinflammation: a Novel Hallmark in Lafora Progressive Myoclonus Epilepsy That Progresses with Age. Mol Neurobiol 57(3):1607–1621
23. Munoz-Ballester C, Berthier A, Viana R, Sanz P (2016) Homeostasis of the astrocytic glutamate transporter GLT-1 is altered in mouse models of Lafora disease. Biochim Biophys Acta 1862(6):1074–1083

24. Munoz-Ballester C, Santana N, Perez-Jimenez E, Viana R, Artigas F, Sanz P (2019) In vivo glutamate clearance defects in a mouse model of Lafora disease. Exp Neurol 320:112959
25. Perez-Jimenez E, Viana R, Munoz-Ballester C, Vendrell-Tornero C, Moll-Diaz R, Garcia-Gimeno MA, Sanz P (2021) Endocytosis of the glutamate transporter 1 is regulated by laforin and malin: Implications in Lafora disease. Glia 69(5):1170–1183
26. Garcia-Cabrero AM, Sanchez-Elexpuru G, Serratosa JM, Sanchez MP (2014) Enhanced sensitivity of laforin- and malin-deficient mice to the convulsant agent pentylenetetrazole. Front Neurosci 8:291
27. Duran J, Gruart A, Garcia-Rocha M, Delgado-Garcia JM, Guinovart JJ (2014) Glycogen accumulation underlies neurodegeneration and autophagy impairment in Lafora disease. Hum Mol Genet 23(12):3147–3156
28. Berthier A, Paya M, Garcia-Cabrero AM, Ballester MI, Heredia M, Serratosa JM, Sanchez MP, Sanz P (2016) Pharmacological Interventions to Ameliorate Neuropathological Symptoms in a Mouse Model of Lafora Disease. Mol Neurobiol 53(2):1296–1309
29. Molla B, Heredia M, Sanz P (2021) Modulators of Neuroinflammation Have a Beneficial Effect in a Lafora Disease Mouse Model. Mol Neurobiol 58(6):2508–2522
30. Bissaro M, Moro S (2019) Rethinking to riluzole mechanism of action: the molecular link among protein kinase CK1delta activity, TDP-43 phosphorylation, and amyotrophic lateral sclerosis pharmacological treatment. Neural Regen Res 14(12):2083–2085
31. Kennel P, Revah F, Bohme GA, Bejuit R, Gallix P, Stutzmann JM, Imperato A, Pratt J (2000) Riluzole prolongs survival and delays muscle strength deterioration in mice with progressive motor neuronopathy (pmn). J Neurol Sci 180(1–2):55–61
32. Hunsberger HC, Weitzner DS, Rudy CC, Hickman JE, Libell EM, Speer RR, Gerhardt GA, Reed MN (2015) Riluzole rescues glutamate alterations, cognitive deficits, and tau pathology associated with P301L tau expression. J Neurochem 135(2):381–394
33. Hascup KN, Findley CA, Britz J, Esperant-Hilaire N, Broderick SO, Delfino K, Tischkau S, Bartke A, Hascup ER (2021) Riluzole attenuates glutamatergic tone and cognitive decline in AbetaPP/PS1 mice. J Neurochem 156(4):513–523
34. Rogawski MA, Wenk GL (2003) The neuropharmacological basis for the use of memantine in the treatment of Alzheimer's disease. CNS Drug Rev 9(3):275–308
35. Wenk GL, Parsons CG, Danysz W (2006) Potential role of N-methyl-D-aspartate receptors as executors of neurodegeneration resulting from diverse insults: focus on memantine. Behav Pharmacol 17(5–6):411–424
36. Repossi G, Das UN, Eynard AR (2020) Molecular Basis of the Beneficial Actions of Resveratrol. Arch Med Res 51(2):105–114
37. Meng T, Xiao D, Muhammed A, Deng J, Chen L, He J (2021) Anti-Inflammatory Action and Mechanisms of Resveratrol. Molecules 26(1):1–15
38. Capiralla H, Vingtdeux V, Zhao H, Sankowski R, Al-Abed Y, Davies P, Marambaud P (2012) Resveratrol mitigates lipopolysaccharide- and Abeta-mediated microglial inflammation by inhibiting the

TLR4/NF-kappaB/STAT signaling cascade. J Neurochem 120(3):461–472

39. Venigalla M, Sonego S, Gyengesi E, Sharman MJ, Munch G (2016) Novel promising therapeutics against chronic neuroinflammation and neurodegeneration in Alzheimer's disease. Neurochem Int 95:63–74
40. Garrido-Mesa N, Zarzuelo A, Galvez J (2013) Minocycline: far beyond an antibiotic. Br J Pharmacol 169(2):337–352
41. Moller T, Bard F, Bhattacharya A, Biber K, Campbell B, Dale E, Eder C, Gan L, Garden GA, Hughes ZA, Pearse DD, Staal RG, Sayed FA, Wes PD, Boddeke HW (2016) Critical data-based re-evaluation of minocycline as a putative specific microglia inhibitor. Glia 64(10):1788–1794
42. Li J, Sung M, Rutkove SB (2013) Electrophysiologic biomarkers for assessing disease progression and the effect of riluzole in SOD1 G93A ALS mice. PLoS ONE 8(6):e65976
43. Schmidt J, Schmidt T, Golla M, Lehmann L, Weber JJ, Hubener-Schmid J, Riess O (2016) In vivo assessment of riluzole as a potential therapeutic drug for spinocerebellar ataxia type 3. J Neurochem 138(1):150–162
44. Canistro D, Bonamassa B, Pozzetti L, Sapone A, Abdel-Rahman SZ, Biagi GL, Paolini M (2009) Alteration of xenobiotic metabolizing enzymes by resveratrol in liver and lung of CD1 mice. Food Chem Toxicol 47(2):454–461
45. Singleton RH, Yan HQ, Fellows-Mayle W, Dixon CE (2010) Resveratrol attenuates behavioral impairments and reduces cortical and hippocampal loss in a rat controlled cortical impact model of traumatic brain injury. J Neurotrauma 27(6):1091–1099
46. Molinaro G, Battaglia G, Riozzi B, Di Menna L, Rampello L, Bruno V, Nicoletti F (2009) Memantine treatment reduces the expression of the K(+)/Cl(-) cotransporter KCC2 in the hippocampus and cerebral cortex, and attenuates behavioural responses mediated by GABA(A) receptor activation in mice. Brain Res 1265:75–79
47. Ahmadirad N, Shojaei A, Javan M, Pourgholami MH, Mirnajafi-Zadeh J (2014) Effect of minocycline on pentylenetetrazol-induced chemical kindled seizures in mice. Neurol Sci 35(4):571–576
48. Lalonde R, Strazielle C (2011) Brain regions and genes affecting limb-clasping responses. Brain Res Rev 67(1–2):252–259
49. Guyenet SJ, Furrer SA, Damian VM, Baughan TD, La Spada AR, Garden GA (2010) A simple composite phenotype scoring system for evaluating mouse models of cerebellar ataxia.J Vis Exp(39):e1787
50. Seibenhener ML, Wooten MC (2015) Use of the Open Field Maze to measure locomotor and anxiety-like behavior in mice. J Vis Exp 96:e52434
51. Walf AA, Frye CA (2007) The use of the elevated plus maze as an assay of anxiety-related behavior in rodents. Nat Protoc 2(2):322–328
52. RStudio_Team (2020) RStudio: Integrated development for R. https://wwwrstudiocom/
53. Cohen J (1988) Statistical power analysis for the behavioral sciences (2nd edition). Hillsdale, NJ

54. Kraemer HC, Morgan GA, Leech NL, Gliner JA, Vaske JJ, Harmon RJ (2003) Measures of clinical significance. J Am Acad Child Adolesc Psychiatry 42(12):1524–1529
55. Felsky D, Roostaei T, Nho K, Risacher SL, Bradshaw EM, Petyuk V, Schneider JA, Saykin A, Bennett DA, De Jager PL (2019) Neuropathological correlates and genetic architecture of microglial activation in elderly human brain. Nat Commun 10(1):409
56. Ahonen S, Nitschke S, Grossman TR, Kordasiewicz H, Wang P, Zhao X, Guisso DR, Kasiri S, Nitschke F, Minassian BA (2021) Gys1 antisense therapy rescues neuropathological bases of murine Lafora disease. Brain 144(10):2985–2993
57. Tang B, Frasinyuk MS, Chikwana VM, Mahalingan KK, Morgan CA, Segvich DM, Bondarenko SP, Mrug GP, Wyrebek P, Watt DS, DePaoli-Roach AA, Roach PJ, Hurley TD (2020) Discovery and Development of Small-Molecule Inhibitors of Glycogen Synthase. J Med Chem 63(7):3538–3551
58. Brewer MK, Uittenbogaard A, Austin GL, Segvich DM, DePaoli-Roach A, Roach PJ, McCarthy JJ, Simmons ZR, Brandon JA, Zhou Z, Zeller J, Young LEA, Sun RC, Pauly JR, Aziz NM, Hodges BL, McKnight TR, Armstrong DD, Gentry MS (2019) Targeting Pathogenic Lafora Bodies in Lafora Disease Using an Antibody-Enzyme Fusion. Cell Metab 30(4):689–705e686
59. Austin GL, Simmons ZR, Klier JE, Rondon A, Hodges BL, Shaffer R, Aziz NM, McKnight TR, Pauly JR, Armstrong DD, Vander Kooi CW, Gentry MS (2019) Central Nervous System Delivery and Biodistribution Analysis of an Antibody-Enzyme Fusion for the Treatment of Lafora Disease. Mol Pharm 16(9):3791–3801
60. Israelian L, Wang P, Gabrielian S, Zhao X, Minassian BA (2020) Ketogenic diet reduces Lafora bodies in murine Lafora disease. Neurol Genet 6(6):e533
61. Mohammadzadeh S, Ahangari TK, Yousefi F (2019) The effect of memantine in adult patients with attention deficit hyperactivity disorder. Hum Psychopharmacol 34(1):e2687
62. Dirani M, Nasreddine W, Abdulla F, Beydoun A (2014) Seizure control and improvement of neurological dysfunction in Lafora disease with perampanel. Epilepsy Behav Case Rep 2:164–166
63. Goldsmith D, Minassian BA (2016) Efficacy and tolerability of perampanel in ten patients with Lafora disease. Epilepsy Behav 62:132–135
64. Dasgupta B, Milbrandt J (2007) Resveratrol stimulates AMP kinase activity in neurons. Proc Natl Acad Sci U S A 104(17):7217–7222
65. Porro C, Cianciulli A, Calvello R, Panaro MA (2015) Reviewing the Role of Resveratrol as a Natural Modulator of Microglial Activities. Curr Pharm Des 21(36):5277–5291
66. Gonzalez JC, Egea J, Del Carmen Godino M, Fernandez-Gomez FJ, Sanchez-Prieto J, Gandia L, Garcia AG, Jordan J, Hernandez-Guijo JM (2007) Neuroprotectant minocycline depresses glutamatergic neurotransmission and Ca(2+) signalling in hippocampal neurons. Eur J Neurosci 26(9):2481–2495
67. Lu Y, Yang Y, Chen W, Du N, Du Y, Gu H, Liu Q (2021) Minocycline, but not doxycycline attenuates NMDA-induced [Ca2+]i and excitotoxicity. NeuroReport 32(1):38–43

68. Nie H, Zhang H, Weng HR (2010) Minocycline prevents impaired glial glutamate uptake in the spinal sensory synapses of neuropathic rats. Neuroscience 170(3):901–912

Figures

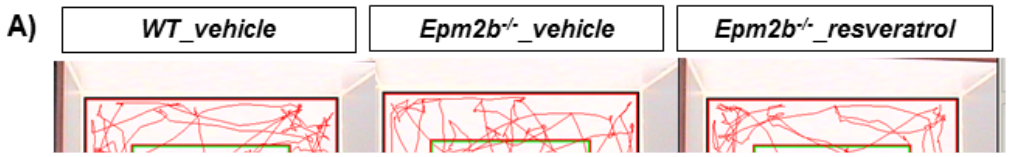

Figure 1

Anxiety-like behavior state in *Epm2b-/-* mice and the therapeutic efficacy of riluzole, memantine, resveratrol, and minocycline treatments. A) Representative tracks were recorded with SMART video system to evaluate the anxiety-like behavior as measured by Open field (see Materials and Methods). **B-E)** % Travelled distance in the center representing the anxiety levels of each animal. Bar graphs show mean ± standard error of the mean (SEM). Individual data points and the comparisons between groups which were $p<0.1$ are indicated. Depending on the normal distribution and homoscedasticity of the data, statistical differences were analyzed, by two-way ANOVA following a Tukey's posthoc to multiple comparisons in (B) and by one-way Kruskal-Wallis following a Dunn's posthoc test to multiple comparisons in (C-E). Statistical significance was defined as $*p<0.05$. A summary of all descriptive (mean ± SEM) and inferential data (all comparisons between groups) is available in Table S1. Treatments

related to glutamatergic transmission are boxed in red and those related to neuroinflammation are in magenta.

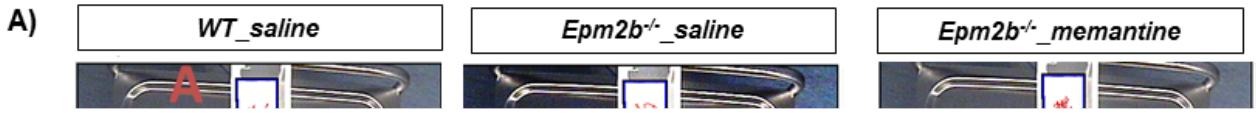

Figure 2

Cognitive state in *Epm2b-/-* mice and the therapeutic efficacy of riluzole, memantine, resveratrol, and minocycline treatments. A) Representative tracks were recorded with SMART video system to evaluate the working memory as measured by y-maze (see Materials and Methods). **B-E)** % of the incomplete alternations representing the attention of staying on the task of each animal. Bar graphs show mean ± standard error of the mean (SEM). Individual data points and the comparisons between groups which were $p<0.1$ are indicated. Depending on the normal distribution and homoscedasticity of the data, statistical differences were analyzed, by two-way ANOVA following a Tukey's posthoc to multiple comparisons in (B, D) and by one-way Kruskal-Wallis following a Dunn's posthoc test to multiple comparisons in (C, E). Statistical significance was defined as $*p<0.05$. A summary of all descriptive (mean ± SEM) and inferential data (all comparisons between groups) is available in Table S1.

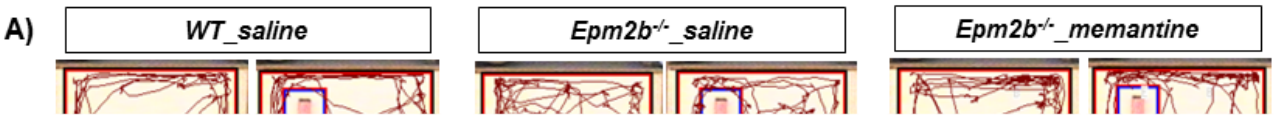

Figure 3

Hyperactivity in *Epm2b-/-* mice and the therapeutic efficacy of riluzole, memantine, resveratrol, and minocycline treatments. A) Representative tracks were recorded with SMART video system to evaluate the spatial location memory as measured by OLM (see Materials and Methods). **B-E)** Total activity time representing the activity levels of each animal. Bar graphs show mean ± standard error of the mean (SEM). Individual data points and the comparisons between groups which were $p<0.1$ are indicated. Depending on the normal distribution and homoscedasticity of the data, statistical differences were analyzed, by two-way ANOVA following a Tukey's posthoc to multiple comparisons in (B) and by one-way Kruskal-Wallis following a Dunn's posthoc test to multiple comparisons in (C-E). Statistical significance was defined as $*p<0.05$. A summary of all descriptive (mean ± SEM) and inferential data (all comparisons between groups) is available in Table S1.

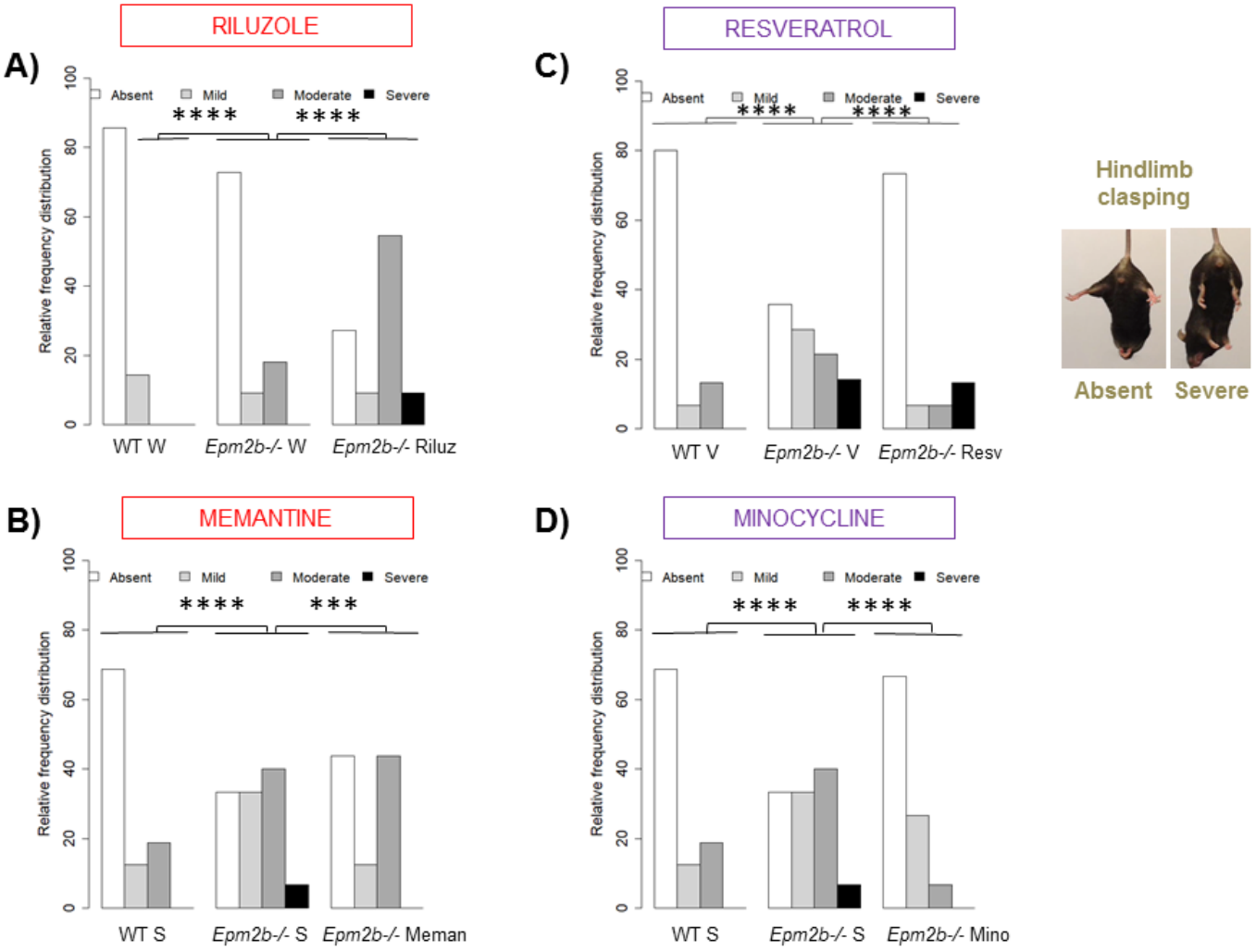

Figure 4

Neurodegenerative state in *Epm2b-/-* mice and the therapeutic efficacy of riluzole, memantine, resveratrol, and minocycline treatments. A-D) Relative frequency distribution of the hindlimb clasping score representing the severity of neurodegenerative signs. Frequency histograms show frequency distribution among 4 scores: absent, mild, moderate, and severe. Statistical differences between groups were analyzed by Pearson's Chi-square test or by Fischer's exact test when sample sizes were zero. Statistical significance was defined as ***p<0.001 and ****p<0.0001. A summary of all contingency tables and inferential data (all comparisons between groups) is available in Table S2.

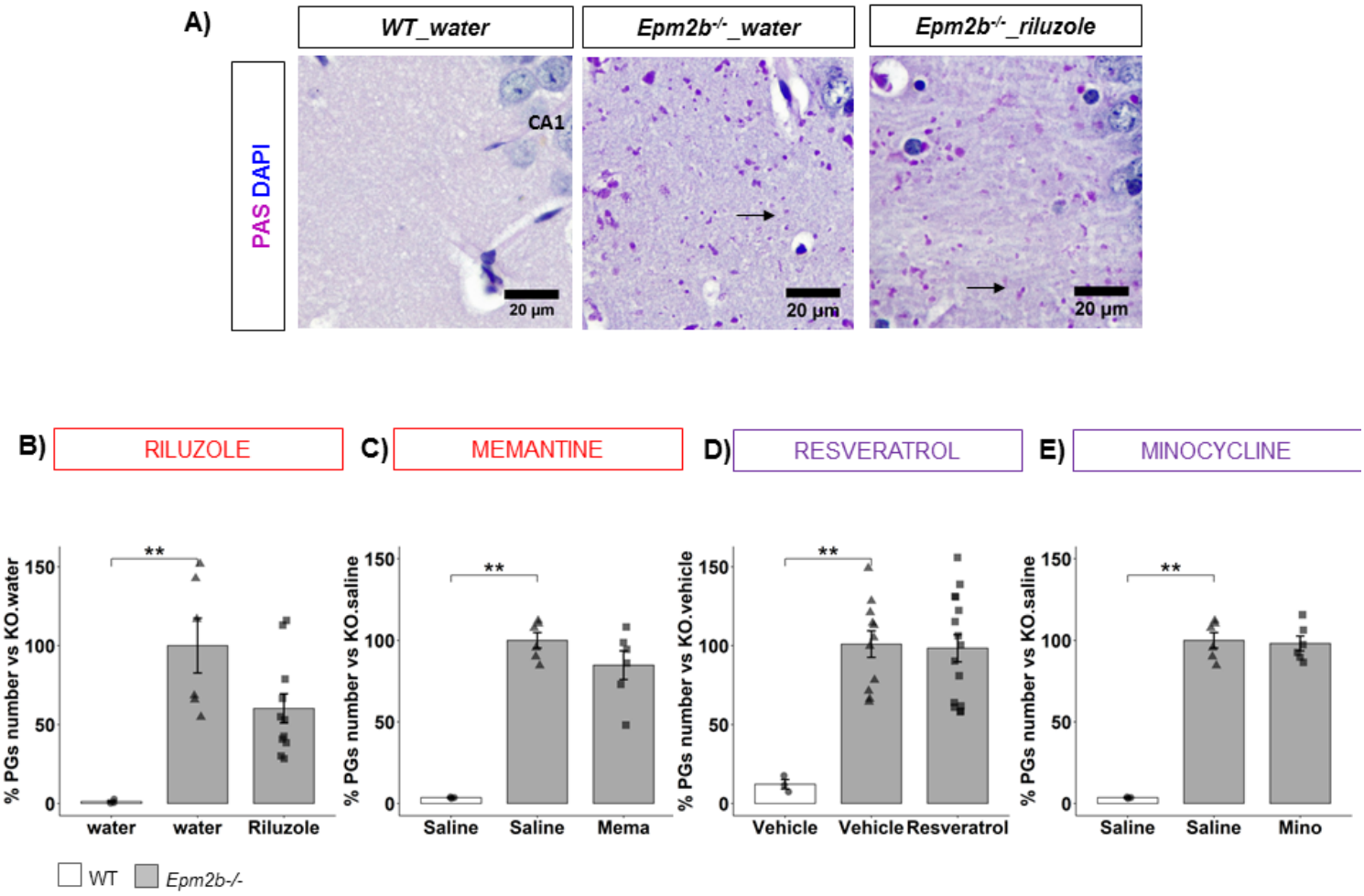

Figure 5

Accumulation of PGs in the hippocampus of *Epm2b-/-* mice and the therapeutic efficacy of riluzole, memantine, resveratrol, and minocycline. **A)** Representative microscopy images of PGs detection (in pink; see also black arrows) in CA1 region of the hippocampus by PAS staining; neural nuclei are in blue. **B-E)** % of PGs number versus the number present in untreated *Epm2b-/-* mice. Bar graphs show mean ± standard error of the mean (SEM). Individual data points and the comparisons between groups which were $p<0.1$ are indicated. Depending on the normal distribution and homoscedasticity of the data, statistical differences were analyzed by one-way ANOVA with Welch's correction following a Tukey's post hoc to multiple comparisons in (B) and by one-way Kruskal-Wallis following a Dunn's post hoc test to multiple comparisons in (C-E). Statistical significance was defined as $**p<0.01$. A summary of all descriptive (mean ± SEM) and inferential data (all comparisons between groups) is available in Table S1. Scale 20 µm.

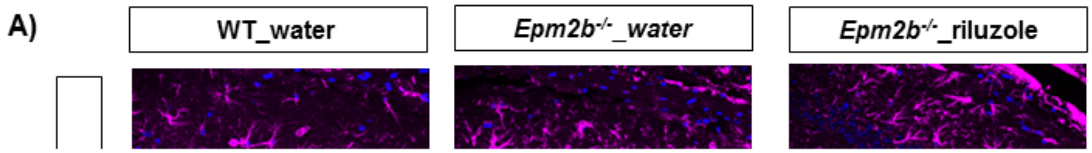

Figure 6

Effect of the different treatments on the reactive astrogliosis of the *Epm2b-/-* mice. A) Representative immunofluorescence confocal micrographs of the CA1 region of the hippocampus. Astrocytes (GFAP staining) are in magenta and DAPI staining of cellular nuclei are in blue. **B-E)** % GFAP area related to the value obtained in untreated *Epm2b-/-* mice, representing the extension of the reactive astrogliosis in the hippocampus. Bar graphs show mean ± standard error of the mean (SEM). Individual data points and the comparisons between groups which were $p<0.1$ are indicated. Depending on the normal distribution and homoscedasticity of the data, statistical differences were analyzed by two-way ANOVA following a Tukey's post hoc to multiple comparisons in (D) and by one-way Kruskal-Wallis following a Dunn's post hoc test to multiple comparisons in (B, C, E). Statistical significance was defined as $**p<0.01$. A summary of all descriptive (mean ± SEM) and inferential data (all comparisons between groups) is available in Table S1. Scale 75 µm.

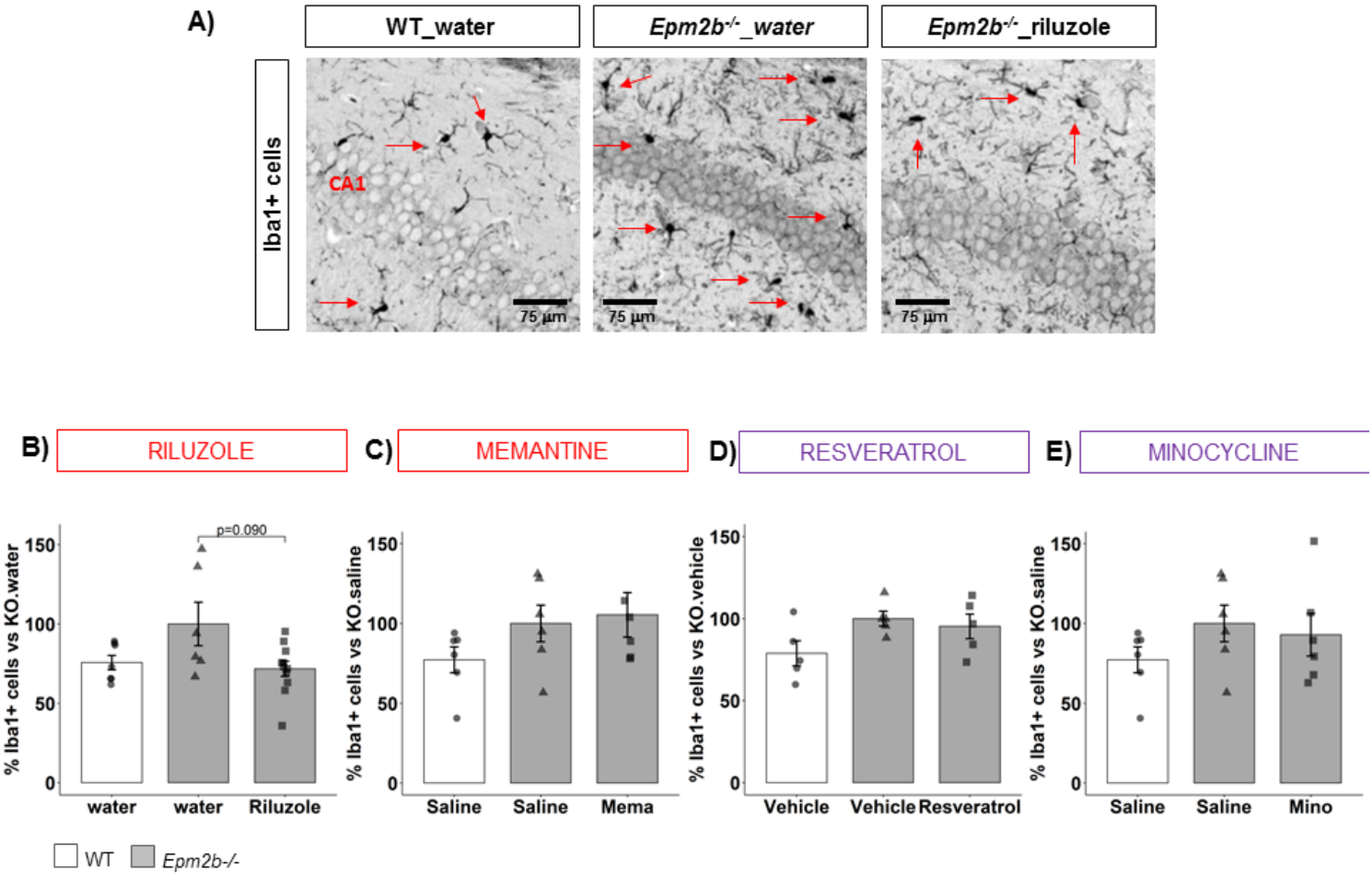

Figure 7

Effect of the different treatments on the reactive microglia in the hippocampus of *Epm2b-/-* mice. A) Representative immunofluorescence confocal micrographs of Iba1 (in gray) to appreciate the remarkable morphological changes in microglia in *Epm2b-/-* mice (see red arrows); **B-E) %** Iba1 positive cells related to the value obtained in untreated *Epm2b-/-* mice, representing the extension of the reactive microglia in the hippocampus with morphological changes. Bar graphs show mean ± standard error of the mean (SEM). Individual data points and the comparisons between groups which were $p<0.1$ are indicated. Depending on the normal distribution and homoscedasticity of the data, statistical differences were analyzed by two-way ANOVA following a Tukey's post hoc to multiple comparisons in (C-E) and by one-way Kruskal-Wallis following a Dunn's post hoc test to multiple comparisons in (B). A summary of all descriptive (mean ± SEM) and inferential data (all comparisons between groups) is available in Table S1. Scale 75 µm.

Supplementary Files

This is a list of supplementary files associated with this preprint. Click to download.

- SupplementaryinformationFig.S1TablesS1andS2.pdf